

A Capture-Recapture Approach to Facilitate Causal Inference for a Trial-eligible Observational Cohort

Lin Ge^{1,2}, Yuzi Zhang³, Lance A. Waller¹, Robert H. Lyles¹

¹ Department of Biostatistics and Bioinformatics, Rollins School of Public Health,
Emory University, Atlanta, GA, U.S.A

² Department of Epidemiology and Biostatistics, T.H. Chan School of Public Health,
Harvard University, Boston, MA, U.S.A

³ Division of Biostatistics, College of Public Health,
Ohio State University, Columbus, OH, U.S.A

Abstract

We extend recently proposed design-based capture-recapture (CRC) methods for prevalence estimation among registry participants, in order to enable causal inference among a trial-eligible target population. The design for CRC analysis integrates an observational study cohort with a randomized trial involving a small representative study sample, and enhances the generalizability and transportability of the findings. We show that a novel CRC-type estimator derived via multinomial distribution-based maximum-likelihood exploits the design to deliver benefits in terms of validity and efficiency for comparing the effects of two treatments on a binary outcome. The design also unlocks a direct standardization-type estimator that allows efficient estimation of general means (e.g., for continuous outcomes such as biomarker levels) under a specific treatment. This provides an avenue to compare treatment effects within the target population in a more comprehensive manner. For inference, we recommend using a tailored Bayesian credible interval approach to improve coverage properties in conjunction with the proposed CRC estimator when estimating binary treatment effects, and a bootstrap percentile interval approach for use with continuous outcomes. Simulations demonstrate the validity and efficiency of the proposed estimators under the CRC design. Finally, we present an illustrative data application comparing Anti-S Antibody seropositive response rates for two major Covid-19 vaccines using an observational cohort from Tunisia.

Keywords: Capture-Recapture methods, Causal inference, Generalizability and transportability, Standardization

Capture-Recapture Approach to Facilitate Causal Inference for a Trial-eligible Observational Cohort

1. Introduction

Observational studies are widely used in various fields, such as epidemiology and the social sciences, as they facilitate the collection of cohort data for analysis. However, making causal conclusions based on observational data is well known to be problematic due to the lack of random experimental assignment to treatments, resulting in confounding bias.¹ To reduce bias in observational studies, methods such as propensity matching,² inverse probability weighting (IPW),³ or augmented IPW (AIPW)³ are often used in practice. On the other hand, randomized trials offer favorable properties with respect to internal validity⁴ and unbiased estimation, although generalizing the conclusions to all eligible individuals can be challenging.^{5,6} Many studies focus on addressing the generalizability from randomized trial results to broader target populations.⁷⁻⁹

In this article, we tailor capture-recapture (CRC) methods toward the extension of causal inference from an observational cohort to larger registered trial-eligible target populations. CRC methodology was originally developed for use in ecological studies seeking to estimate wildlife populations in a specific area,^{10,11} but has also been applied in numerous epidemiological and public health research studies estimating case counts or prevalence of diseases¹²⁻¹⁴ and conditions.¹⁵ Key to CRC analysis is estimating the missing count of individuals “caught” by none of the capture efforts, enabling an overall count assessment from the sum of the observed count and the estimated missing count. For treatment effect evaluation, CRC analysis can be adapted to estimate the mean of a binary outcome (e.g., for prevalence estimation) or a continuous outcome¹⁶

(e.g., a biomarker level) in a closed target population, thus potentially making CRC tools useful for addressing popular causal inference questions.

In this article, the causal inference setting is conceptualized within a two-stream CRC design framework. While sensitivity and uncertainty analyses have been explored,^{17,18} the implementation of CRC analysis based on two data streams is generally problematic without a key independence assumption known as the Lincoln-Petersen, or “LP”, condition.¹⁹ It assumes that the two data streams utilized in the CRC analysis operate independently of each other, at least at a population level. However, in practice, it is well known that such independence is often questionable and can lead to biased estimation if violated.^{20,21} To address this issue, several articles^{19,22} have discussed how the independence condition can be satisfied by conducting a principled random sample from the target population that is designed to be independent of a second established surveillance effort. One such design-based approach recently has been implemented within CRC analysis^{16,23,24} when the target population consists of a list or registry amenable to random sampling, providing a so-called “anchor stream” of representative data that augments a non-representative sample. Because a key association parameter becomes known by design, this approach yields an estimator of population size that is generally far more precise than traditional CRC estimators under the LP conditions.²¹ In this article, we focus on this design-based approach and implement the same CRC analysis framework more generally, based on embedding a randomized trial within a larger observational cohort by collecting a relatively small random sample of members of a registered clinic population. Those selected are randomized to one of two available treatments, with the goal of comparing their success rates in a way that generalizes to the entire target population while also making use of information from arbitrarily non-representative observational data on subjects who utilized the treatment that they or their provider selected.

These methods that we propose are based on the clinical equipoise assumption,^{25,26} which stipulates that there is no established preference for one treatment over another in a given population. This setting is common in trial design (e.g., when studying the repurposing of approved drugs) and has been leveraged, for example, to compare option A and option B drug regimens for prevention of mother-to-child transmission of HIV (PMTCT).²⁷ We assume that two treatments in equipoise are being evaluated among a closed target population of individuals eligible for both treatments. An observational study is to be initiated (forming the basis for the first data stream), and a small randomized trial is essentially designed to be embedded in order to obtain treatment-specific outcomes for a representative subset of participants selected from the target population^{28,29} using either a simple or stratified random sampling approach. The CRC method combines information from both the observational and experimental data, achieving dual goals: improving the reliability of the observational evidence via the randomized trial data, and increasing the statistical efficiency of the randomized trial component via the observational information.¹ This study design is detailed as follows, and visualized in Figure 1.

- *We assume a closed trial-eligible participant population with a known size, within which both equipoised treatment options (A and B) are to be made available to participants. Individuals who could not feasibly be administered one or both treatments of interest (e.g., due to indications associated with risk or tolerability) are first removed from the target population.*
- *The medical providers of the participants determine an assignment of treatment (A or B). This assignment may be associated with physician preference (possibly driven by ties to the manufacturer) and driven by participant characteristics (e.g., clinical data, insurance status, etc.) that could be related to the probability of treatment response. This forms the*

basis of the observational cohort subject to initial assigned treatment selection by the provider, which we hereafter refer to as Stream 1 (or S1). Note that the observational cohort is a subset of the target population in the study.

- Before initiating the assigned treatment (A or B) for each person by the provider, we collect a (likely relatively small in comparison to the observational cohort) random sample from the target population. Each selected participant is then randomized to either receive A or B, forming the basis for the sampling-based component that we denote as Stream2 (or S2). Importantly, we assume the buy-in of the observational cohort and their providers. That is, if a patient is selected in the random sample and randomized to the treatment not initially chosen, their provider will administer the randomly prescribed treatment. This is referred to as a “label-switching” strategy in the following sections; however, it is important to note that all other patients will keep the treatment initially assigned by the provider.

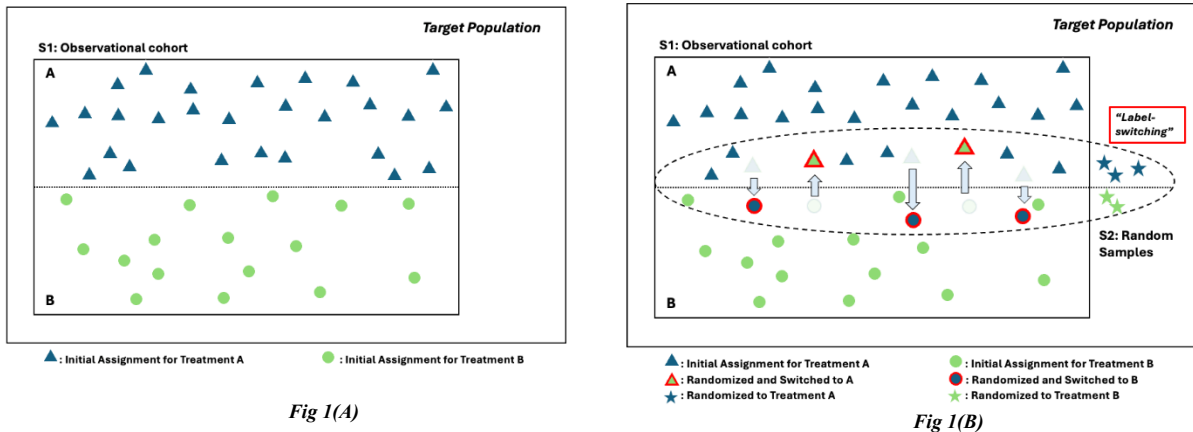


Figure 1 Visualization Diagrams Illustrating the Study Design Details Under the “label-switching” Strategy. Fig 1(A) shows the initial assigned treatment (A or B) in the observational cohort (Stream 1, or S1), as determined by the medical providers. Fig 1(B) indicates the final treatment assignments, incorporating provide “buy-in” for randomly selected individuals from the target population (Stream 2, or S2). The red outlines describe the “label-switching” strategy and highlight those randomized and administered to switch to a different treatment from the initial assigned selection. The star symbols represent new participants with randomized treatment selection by Stream 2 from the target population, who did not receive initial assignment in the observational cohort.

2. Methods

2.1 Targets of Inference and Notation

In what follows, we assume the design strategy described above to be in effect along with the accompanying caveats. Let \mathcal{T} be the set of treatments of interest to be assessed in the CRC analysis. For each treatment A (or B) $\in \mathcal{T}$, we use the random variable Y^A (or Y^B) to denote the counterfactual outcome under intervention to receive treatment A (or B).^{30–32} For simplicity, we only consider two treatments (A and B) here; however, an extension to more treatments can be made naturally.

We use the following notation to facilitate the description of the proposed method: N_{tot} is the known total size of the closed target population, and $i = 1, 2, \dots, N_{tot}$ indexes each individual in the population; $S_i^{(1)}, S_i^{(2)}$ are the indicators for being observed in the observational cohort or the anchor stream respectively; $T_i^{(1)}$ is the treatment assignment in the observational cohort study, $T_i^{(2)}$ is the randomized treatment assignment in the anchor stream, T_i is the final treatment assignment after the “*label-switching*” strategy (i.e., $T_i = T_i^{(2)}$ if the patient has an assigned treatment $T_i^{(2)}$ from the anchor stream; otherwise $T_i = T_i^{(1)}$). Note that T_i can be a missing value if neither of the two streams assigns a treatment. Y_i is the observed binary outcome to indicate treatment response; this is extended to the case of continuous outcome treatment response evaluation in section 2.5.

We are interested in performing causal inference regarding the comparison of treatment effects with respect to the entire target population based on the observed CRC data from Streams 1 (observational cohort) and 2 (anchor stream). To better visualize the data from this study design, we use Figure 2 to illustrate the CRC observations. In general, the targets of inference are the outcome variable means (treatment effects) $\mu_A = E(Y^A)$ for each $A \in \mathcal{T}$, and the Average Treatment Effects (*ATE*), i.e., $E(Y^A - Y^B)$ for any pair of treatments $A, B \in \mathcal{T}$. While these goals

can be met based on the representative sampling-based Stream 2 alone, a key objective is to also utilize the (likely much larger but arbitrarily non-representative) Stream 1 sample in the interest of improved precision.

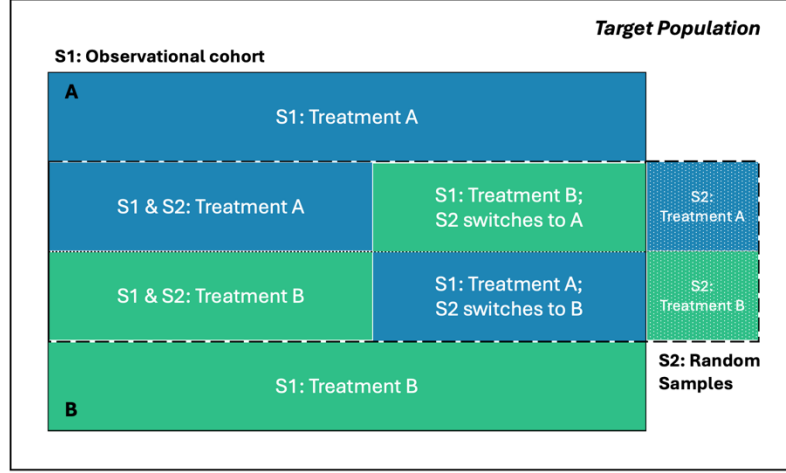


Figure 2 Visualization Diagram illustrating the CRC observations based on the study design.

2.2 Existing Classical Estimators for Treatment Effect Estimation

The “anchor stream” design with label switching ensures that the sample subject to randomization in Stream 2 is drawn “agnostically” (i.e., independently) with respect to the ultimate Stream 1 observational study participant cohort subset of the target population. As Stream 2 introduces representative samples of the target population assigned to each treatment, a simple and defensible estimator is immediately available to satisfy the identifiability of the treatment effect, i.e., of $\mu(A) = E(Y^A) = E(Y|T = A) = E(Y|T = A, S^{(2)} = 1)$ for each $A \in \mathcal{T}$. The random sampling-based estimator is given as follows:

$$\hat{\mu}_{RS}(A) = \frac{1}{n_A} \sum_i I(T_i^{(2)} = A) Y_i, \quad \hat{V}(\hat{\mu}_{RS}(A)) = \frac{\hat{\mu}_{RS}(A) (1 - \hat{\mu}_{RS}(A))}{n_A} \quad (1)$$

where $n_A = \sum_i I(T_i^{(2)} = A)$ and $A \in \mathcal{T}$. Note that in this study setting, we assume no finite population correction (FPC) to the variance in (1), in contrast to previous studies^{16,23,24,33} of anchor stream-based disease prevalence estimation that incorporated FPC effects. This aligns with the implications of sampling repetition in the current setting, where the total population and the S1 and S2 sample sizes remain fixed but the number of individuals responding to treatment varies.

Alternatively, note that implementation of the anchor stream design fully justifies the Lincoln-Petersen condition,^{34,35} so that the classical LP and Chapman CRC estimators are applicable.³⁴⁻³⁶ One focus of this article is on estimating the total number responding as well as the response rate (i.e., treatment effect) for a given treatment $A \in \mathcal{T}$, which could be done via (1) or via simple CRC estimation based on the three observed cell counts in **Table 1**.^{25,38} Specifically, n_{11} is the number of individuals who respond to treatment A among those who receive treatment A both in the initial assignment in Stream 1 and in the randomization in Stream 2 (i.e., $T^{(1)} = A$, and $T^{(2)} = A$). The cell count n_{10} is the number of individuals who respond to treatment A among those who receive treatment A in the initial assignment in Stream 1 but were not selected for randomization in Stream 2 (i.e., $T^{(1)} = A$, and $S^{(2)} = 0$). Finally, n_{01} is the number of individuals who respond to treatment A among those who were not assigned to treatment A in Stream 1 but were selected for randomization to treatment A in Stream 2. Note that n_{01} includes both those individuals who did not receive an initial assignment but were randomized for treatment A in Stream 2 (i.e., $S^{(1)} = 0$, and $T^{(2)} = A$), and those who received initial assignment for treatment B but were switched to treatment A due to the randomization assignment in Stream 2 (i.e., $T^{(1)} = B$, and $T^{(2)} = A$). Note that the treatment effect can be calculated by averaging across the known effective total population size $N_{tot}^{(A)}$ of the target population N_{tot} , which is equal to N_{tot} minus the number of individuals selected and randomized to treatment B in Stream 2. That is, the anchor

stream sampling procedure wherein individuals are first randomly chosen for Stream 2 and subsequently randomized for both treatments, is equivalent to a process in which individuals are randomly chosen for treatment A from a subpopulation that omits those randomly chosen for treatment B in Stream 2.

It follows that one direct and valid alternative to (1) for estimating the proportion of the total population who would respond to treatment A is to use the well-known Chapman estimator^{22,36}. The estimated treatment effect $\hat{\mu}_{Chap}(A)$ for a given treatment $A \in \mathcal{T}$ and its estimated variance are given as follows:

$$\hat{\mu}_{Chap}(A) = \frac{1}{N_{tot}^{(A)}} \left[\frac{(n_{1.} + 1)(n_{.1} + 1)}{n_{11} + 1} - 1 \right], \quad \hat{v}(\hat{\mu}_{Chap}(A)) = \frac{1}{N_{tot}^{(A)2}} \left[\frac{(n_{1.} + 1)(n_{.1} + 1)n_{1.}n_{.1}}{(n_{11} + 1)^2(n_{11} + 2)} \right] \quad (2)$$

Wald-type confidence intervals (CIs) based on the Chapman estimate and its variance in (2) are known to provide unsatisfactory coverage in many CRC settings under the LP conditions. Therefore, we summarize results based on a more reliable transformed logit CI³⁷ in our simulation studies to follow.

Table 1 Responder Counts for Two-Stream Capture-Recapture for One Treatment $T = A \in \mathcal{T}$

	Observed to respond to treatment A in Stream 2 (i.e., $S^{(2)} = 1$)		
Observed to respond to treatment A in Stream 1 (i.e., $S^{(1)} = 1$)	<i>Yes</i>	<i>No</i>	Total
<i>Yes</i>	n_{11}	n_{10}	$n_{1.}$
<i>No</i>	n_{01}	$n_{00}=?$	
Total	$n_{.1}$		$N=?$

* The effective population size is $N_{tot}^{(A)}$, which omits individuals chosen and randomized for another treatment by Stream 2 from the target population (N_{tot}).

2.3 More Efficient CRC Estimators for Treatment Effect Estimation

An alternative CRC estimator can be developed by utilizing the full observation profile obtained by design in the anchor stream CRC setting with the “label-switching” strategy (see Figure 2).

Specifically, the design yields a maximum-likelihood estimator (MLE) for the effects of both treatments simultaneously, i.e., $\mu(A)$ and $\mu(B)$, under a 17-category multinomial distribution that accounts for each of the N_{tot} members of the registered target population. The details of each observed cell count and its likelihood contribution are in **Table 2**. The derivation for each likelihood contribution is available in Appendix 1 of *Supplementary Document*.

Table 2 Cell Counts and Likelihood Contributions for Observations

Cell Count	Observation Type	Multinomial likelihood contribution
n_1	Sampled in both streams, assigned and randomized to A, $Y = 1$	$p_1 = \xi_A \psi \pi_{s1,A} \phi_A \phi$
n_2	Sampled in both streams, assigned and randomized to A, $Y = 0$	$p_2 = \xi_A \psi (1 - \pi_{s1,A}) \phi_A \phi$
n_3	Sampled and assigned treatment A in Stream 1, but not sampled in Stream 2, $Y = 1$	$p_3 = (1 - \psi) \pi_{s1,A} \phi_A \phi$
n_4	Sampled and assigned treatment A in Stream 1, but not sampled in Stream 2, $Y = 0$	$p_4 = (1 - \psi) (1 - \pi_{s1,A}) \phi_A \phi$
n_5	Sampled and assigned treatment B in Stream 1; sampled in Stream 2, randomized and switched label to A, $Y = 1$	$p_5 = \xi_A \psi \pi_{s1,B,A} (1 - \phi_A) \phi$
n_6	Sampled and assigned treatment B in Stream 1; sampled in Stream 2, randomized and switched label to A, $Y = 0$	$p_6 = \xi_A \psi (1 - \pi_{s1,B,A}) (1 - \phi_A) \phi$
n_7	Sampled in both streams, assigned and randomized to B, $Y = 1$	$p_7 = (1 - \xi_A) \psi \pi_{s1,B} (1 - \phi_A) \phi$
n_8	Sampled in both streams, assigned and randomized to B, $Y = 0$	$p_8 = (1 - \xi_A) \psi (1 - \pi_{s1,B}) (1 - \phi_A) \phi$
n_9	Sampled and assigned treatment B in Stream 1, but not sampled in Stream 2, $Y = 1$	$p_9 = (1 - \psi) \pi_{s1,B} (1 - \phi_A) \phi$
n_{10}	Sampled and assigned treatment B in Stream 1, but not sampled in Stream 2, $Y = 0$	$p_{10} = (1 - \psi) (1 - \pi_{s1,B}) (1 - \phi_A) \phi$
n_{11}	Sampled and assigned treatment A in Stream 1; sampled in Stream 2, randomized and switched label to B, $Y = 1$	$p_{11} = (1 - \xi_A) \psi \pi_{s1,A,B} \phi_A \phi$
n_{12}	Sampled and assigned treatment in A Stream 1; sampled in Stream 2, randomized and switched label to B, $Y = 0$	$p_{12} = (1 - \xi_A) \psi (1 - \pi_{s1,A,B}) \phi_A \phi$
n_{13}	Not sampled in Stream 1; sampled in Stream 2 and randomized to A, $Y = 1$	$p_{13} = \xi_A \psi \pi_{s1,NA,A} (1 - \phi)$
n_{14}	Not sampled in Stream 1; sampled in Stream 2 and randomized to A, $Y = 0$	$p_{14} = \xi_A \psi (1 - \pi_{s1,NA,A}) (1 - \phi)$
n_{15}	Not sampled in Stream 1; sampled in Stream 2 and randomized to B, $Y = 1$	$p_{15} = (1 - \xi_A) \psi \pi_{s1,NA,B} (1 - \phi)$
n_{16}	Not sampled in Stream 1; sampled in Stream 2 and randomized to B, $Y = 0$	$p_{16} = (1 - \xi_A) \psi (1 - \pi_{s1,NA,B}) (1 - \phi)$

n_{17}	Not sampled in Stream 1; not sampled in Stream 2	$p_{17} = (1 - \psi)(1 - \phi)$
----------	--	---------------------------------

*Connections with **Table 1**: $n_{11}^{(A)} = n_1$, $n_{10}^{(A)} = n_3$, and $n_{01}^{(A)} = n_5 + n_{13}$; $n_{11}^{(B)} = n_7$, $n_{10}^{(B)} = n_9$, and $n_{01}^{(B)} = n_{11} + n_{15}$

The likelihood contributions given in **Table 2** are based on defining the parameters, $\phi = \Pr(\text{Sampled in Stream 1})$, $\phi_A = \Pr(\text{Assigned treatment } A \mid \text{sampled in Stream 1})$, $\pi_{s1,A} = \Pr(Y = 1 \mid \text{Sampled and assigned treatment } A \text{ in Stream 1, and received } A)$, $\pi_{s1,B,A} = \Pr(Y = 1 \mid \text{Sampled and assigned treatment } B \text{ in Stream 1, but received } A)$, $\pi_{s1,NA,A} = \Pr(Y = 1 \mid \text{Not sampled in Stream 1, but received } A)$, $\pi_{s1,B} = \Pr(Y = 1 \mid \text{Sampled and assigned treatment } B \text{ in Stream 1, and received } B)$, $\pi_{s1,A,B} = \Pr(Y = 1 \mid \text{Sampled and assigned treatment } A \text{ in Stream 1, but received } B)$, $\pi_{s1,NA,B} = \Pr(Y = 1 \mid \text{Not sampled in Stream 1, but received } B)$. Additionally, there are two more parameters $\psi = \Pr(\text{Sampled in Stream 2})$ and $\xi_A = \Pr(\text{Randomized to } A \mid \text{Sampled in Stream 2})$ that can be treated as known. We set $\xi_A = 50\%$ here to reflect an assumption of balanced treatment assignment via randomization, but it can be altered to accommodate unbalanced scenarios targeted by design. Letting p_j denote the likelihood contribution corresponding to the j th cell, the vector of cell counts can be modeled as a multinomial sample with likelihood proportional to $\prod_{j=1}^{17} p_j$, i.e.,

$$(n_1, n_2, \dots, n_{17}) \sim \text{multinomial}(N_{tot}; p_1, p_2, \dots, p_{17})$$

All parameters in **Table 2** are identifiable, and the MLEs of each parameter as well as the corresponding estimated variances are derivable in closed form (see Appendix 2) as follows:

- $\hat{\phi} = \frac{N_1}{N_{tot}}$, $\hat{V}(\hat{\phi}) = \frac{\hat{\phi}(1-\hat{\phi})}{N_{tot}}$, where $N_1 = N_{tot} - (n_{13} + n_{14} + n_{15} + n_{16} + n_{17})$
- $\hat{\phi}_A = \frac{N_{1,A}}{N_1}$, $\hat{V}(\hat{\phi}_A) = \frac{\hat{\phi}_A(1-\hat{\phi}_A)}{N_1}$, where $N_{1,A} = n_1 + n_2 + n_3 + n_4 + n_{11} + n_{12}$
- $\hat{\pi}_{s1,A} = \frac{n_1 + n_3}{n_1 + n_2 + n_3 + n_4}$, $\hat{V}(\hat{\pi}_{s1,A}) = \frac{\hat{\pi}_{s1,A}(1-\hat{\pi}_{s1,A})}{n_1 + n_2 + n_3 + n_4}$
- $\hat{\pi}_{s1,B,A} = \frac{n_5}{n_5 + n_6}$, $\hat{V}(\hat{\pi}_{s1,B,A}) = \frac{\hat{\pi}_{s1,B,A}(1-\hat{\pi}_{s1,B,A})}{n_5 + n_6}$

- $\hat{\pi}_{s1_NA,A} = \frac{n_{13}}{n_{13}+n_{14}}, \hat{V}(\hat{\pi}_{s1_NA,A}) = \frac{\hat{\pi}_{s1_NA,A}(1-\hat{\pi}_{s1_NA,A})}{n_{13}+n_{14}}$
- $\hat{\pi}_{s1,B} = \frac{n_7+n_9}{n_7+n_8+n_9+n_{10}}, \hat{V}(\hat{\pi}_{s1,B}) = \frac{\hat{\pi}_{s1,B}(1-\hat{\pi}_{s1,B})}{n_7+n_8+n_9+n_{10}}$
- $\hat{\pi}_{s1_A,B} = \frac{n_{11}}{n_{11}+n_{12}}, \hat{V}(\hat{\pi}_{s1_A,B}) = \frac{\hat{\pi}_{s1_A,B}(1-\hat{\pi}_{s1_A,B})}{n_{11}+n_{12}}$
- $\hat{\pi}_{s1_NA,B} = \frac{n_{15}}{n_{15}+n_{16}}, \hat{V}(\hat{\pi}_{s1_NA,B}) = \frac{\hat{\pi}_{s1_NA,B}(1-\hat{\pi}_{s1_NA,B})}{n_{15}+n_{16}}$

Of special note and convenience here is the fact that the covariances among the 8 closed-form MLEs above are all equal to zero under the multinomial model.

The estimated treatment effects under each treatment option (generalizable to the entire target population) are evaluated as follows:

$$\hat{\mu}_{CRC}(A) = \hat{\pi}_{s1,A}\hat{\phi}_A\hat{\phi} + \hat{\pi}_{s1,B,A}(1-\hat{\phi}_A)\hat{\phi} + \hat{\pi}_{s1_NA,A}(1-\hat{\phi}) \quad (3)$$

$$\hat{\mu}_{CRC}(B) = \hat{\pi}_{s1,B}(1-\hat{\phi}_A)\hat{\phi} + \hat{\pi}_{s1_A,B}\hat{\phi}_A\hat{\phi} + \hat{\pi}_{s1_NA,B}(1-\hat{\phi}) \quad (4)$$

The variance estimators for (3) and (4) are readily evaluated via the multivariate delta method, facilitated by available closed forms for the variances of the individual estimated parameters. Details about the derivations are available in Appendix 3 of the *Supplementary Document*. To achieve better coverage rates for interval estimation, we propose a Bayesian credible interval approach in the following section to improve upon the ordinary Wald-type confidence interval.

One advantage of this CRC estimator based on the multinomial distribution underlying **Table 2** is that both of the treatment effects can be estimated simultaneously. To connect directly with past work on use of the anchor stream design for prevalence estimation, one can also derive maximum likelihood estimators corresponding to each treatment based on two separate condensed versions of **Table 2**. This involves collapsing the observation profiles in terms of a single treatment and denoting those who were randomized to the other treatment as “not sampled in either stream”, as in Table 2 of Lyles et al.²³ This yields alternative estimates of the treatment effects for both treatments as follows:

$$\hat{\mu}_{\hat{\Psi}}(A) = \frac{1}{N_{tot}^{(A)}} \left[n_{11,A} + n_{10,A} + \frac{n_{01,A}}{\hat{\Psi}(A)} \right] \quad (5)$$

$$\hat{\mu}_{\hat{\Psi}}(B) = \frac{1}{N_{tot}^{(B)}} \left[n_{11,B} + n_{10,B} + \frac{n_{01,B}}{\hat{\Psi}(B)} \right] \quad (6)$$

where $\hat{\Psi}(A) = \frac{n_5 + n_6 + n_{13} + n_{14}}{N_{tot}^{(A)} - (n_1 + n_2 + n_3 + n_4)}$, $\hat{\Psi}(B) = \frac{n_{11} + n_{12} + n_{15} + n_{16}}{N_{tot}^{(B)} - (n_7 + n_8 + n_9 + n_{10})}$, $N_{tot}^{(A)} = N_{tot} - (n_7 + n_8 + n_{11} + n_{12} + n_{15} + n_{16})$ and $N_{tot}^{(B)} = N_{tot} - (n_1 + n_2 + n_5 + n_6 + n_{13} + n_{14})$. Note that the connection between the observed cell counts in **Table 1** and **Table 2** is given in the footnote of **Table 2**. The accompanying variance estimators for (5) and (6) are evaluated through the multivariate delta method based on the condensed table specific to each single treatment.²³

2.4 A Bayesian Credible Interval Approach

The performance of Wald-type confidence intervals (CIs) in binomial/multinomial settings has been shown to be unsatisfactory in numerous studies,^{38,39} especially when the sample size is small. In this article, we propose a Bayesian credible interval approach based on a weakly informative Jeffreys prior on the full multinomial model associated with **Table 2** in an effort to provide more reliable coverage compared to Wald-type CIs as companions to the novel multinomial distribution-based CRC estimator introduced above. The approach has connections with similar proposals made in conjunction with the original anchor stream design for estimating a prevalent case count^{16,23}, except in this case the administration of treatment followed by outcome assessment allows one to rely upon the typical multinomial variance-covariance matrix without concern about finite population sampling.

Our proposed credible interval approach begins with a Jeffreys *Dirichlet*(0.5, 0.5, ..., 0.5) prior for the 17 cell probabilities associated with **Table 2**, yielding the following posterior:

$$(p_1^*, p_2^*, \dots, p_{17}^*) | N_{tot} \sim \text{Dirichlet}(n_1 + 0.5, n_2 + 0.5, \dots, n_{17} + 0.5) \quad (7)$$

From each posterior draw via eqn.(7), we derive posterior cell counts $(n_1^*, n_2^*, \dots, n_{17}^*)$ by multiplying by N_{tot} . Thereafter, we evaluate a posterior draw of the ML estimate $\hat{\mu}_{CRC}^*$ for each treatment, by inserting the 17 posterior cell counts into eqns. (3) and (4). Similarly, the alternative ML estimator $\hat{\mu}_{\hat{\phi}}^*$ based on the separate condensed versions of **Table 2** can be mimicked based on eqns. (5) and (6). Subsequently, the proposed approach reports a (2.5th, 97.5th) percentile interval based on the posteriors of the estimated treatment effects, as the Bayesian credible interval to accompany each estimator.

2.5 Extension to Estimate General Means of Continuous Treatment Outcomes

Now we extend our interest to estimating a treatment effect characterized in terms of the mean of a continuous outcome Y , $E(\tilde{Y}^A)$, under intervention via treatment A . For example, the treatment outcome might be a continuous variable (e.g., a continuous biomarker level or the change in such a level). In general, the direct standardization method⁴⁰ is a useful approach to estimate means or rates based on stratified sampling with known or estimable sampling rates within strata. Due to the anchor stream design, stratification can be based on three parts that are same as in the partition represented in eqns. (3) and (4). In this case, a tailored direct standardization-type estimator¹⁶ is unlocked for the mean of Y for each treatment $A \in \mathcal{T}$ as follows:

$$E(\tilde{Y}^A) = \bar{y}_{s1,A} \hat{p}_{s1,A} + \bar{y}_{s1,B,A} \hat{p}_{s1,B,A} + \bar{y}_{s1,NA,A} \hat{p}_{s1,NA,A} \quad (8)$$

where $\hat{p}_{s1,A} = \hat{\phi}_A \hat{\phi}$, $\hat{p}_{s1,B,A} = (1 - \hat{\phi}_A) \hat{\phi}$, $\hat{p}_{s1,NA,A} = (1 - \hat{\phi})$ and $\bar{y}_{s1,A} = E(\tilde{Y} | \text{Sampled and assigned treatment } A \text{ in Stream 1, and received } A)$, $\bar{y}_{s1,B,A} = E(\tilde{Y} | \text{Sampled and assigned treatment } B \text{ in Stream 1, but received } A)$, $\bar{y}_{s1,NA,A} = E(\tilde{Y} | \text{Not sampled in Stream 1, but received } A)$. The estimators $\hat{\phi}_A$ and $\hat{\phi}$ are evaluated based on the MLEs provided in Section 2.3 and the expectations are estimated based on sample means of each subpopulation.

Regarding inference on the general mean of a continuous outcome, we propose employing a standard bootstrap approach⁴¹ on the observed data to assess both the standard error (SE) and the bootstrap percentile intervals. To elaborate, we initiated the process with the observed data records of all individuals identified at least once from either the observational cohort or the anchor stream (i.e., $S_i^{(1)} = 1$ and/or $S_i^{(2)} = 1$ for all i in the target population). We then randomly draw M bootstrap samples with replacement from this list of individuals. For each bootstrap sample, we evaluate the estimator using eqn. (8) and subsequently calculate the standard error and 95% percentile interval.

3. Simulation Studies

In this section, we present two sets of simulation studies to compare the performance of each estimator introduced in the previous section, assessing the binary treatment effect estimators and the proposed general mean estimator in the case of continuous treatment outcomes.

With sampling under the anchor stream design, we generate the data based on a hypothetical scenario that mimics a comparison between experimental treatments A and B among a closed target population. First, we generate a population of size $N_{tot} = (500; 1,000; 5,000)$ and stratify it into two groups (40% vs 60%) based on a binary characteristic or trait. For Stream 1, we randomly include 70% of individuals from stratum 1 and 90% from stratum 2 to form the observational cohort. We initially simulate the assigned treatment by the provider based on the existing strata categories. Specifically, 30% of individuals in stratum 1 choose treatment A and 80% of individuals in stratum 2 choose treatment A , resulting in cohort data collected from Stream 1. Before initiating the “chosen” treatment for each individual, we simulate Stream 2 as a random sample from the target population through a range of sampling rates, i.e., $p_2 = (5\%, 10\%, 20\%)$

and evenly assign the treatment at random to the individuals in it. All individuals who were not part of the random sample in Stream 2, or who were part of that sample and randomized to the same treatment that they chose in Stream 1, keep their initial assigned treatment. However, for the small contingent of “unlucky” ones, a switch is made to the other treatment (as per the “*label-switching*” strategy).

For the first simulation study assessing treatment effects with a binary outcome variable, we generated the treatment outcome (Y) such that 50% of people in stratum 1 and 80% of people in stratum 2 show a response ($Y = 1$) when using treatment A . Conversely, 30% of people in stratum 1 and 70% of people in stratum 2 who receive treatment B demonstrate a response ($Y = 1$). With these specifications, the true outcome means (i.e., response proportions) from treatment A and B are 0.68 and 0.54 respectively, and the effect difference is 0.14. In the tables to follow, we evaluate results for a population size $N_{tot} = 1,000$ based on 2,000 simulation runs per scenario. The proposed Bayesian credible interval is evaluated via 1,000 posterior samples in each iteration. A more expanded set of simulation scenarios examining population sizes of $N_{tot} = 500$ and 5,000 can be found in the Appendix 4 of *Supplementary Document* (Tables S1-S6).

We compare the performance of each estimator in **Table 3**, with a focus on the treatment A response rate. As anticipated, estimation based on Stream 1 only ($\hat{\mu}_1$) yields biased estimates due to the non-representative sampling; the mechanisms behind this would typically be unknown in practice. The other estimators yield negligible empirical bias as expected, benefitting from the anchor stream design. In each setting, both the CRC estimators $\hat{\mu}_{\hat{\varphi}}$ and $\hat{\mu}_{CRC}$ yield greater precision than the random sampling-based estimator ($\hat{\mu}_{RS}$), and the Chapman estimator ($\hat{\mu}_{Chap}$). In particular, the CRC estimator $\hat{\mu}_{\hat{\varphi}}$ demonstrates performance akin to that of the CRC estimator

$\hat{\mu}_{CRC}$; however, the latter exhibits a slightly smaller standard error and narrower interval width, attributed to its utilization of the full set of observations in **Table 2**.

The Wald-type CIs of the CRC estimators $\hat{\mu}_{\Phi}$ and $\hat{\mu}_{CRC}$ tend to be anti-conservative when the sampling rate (p_2) into Stream 2 is small. In contrast, the proposed Bayesian credible interval approach demonstrates a significant improvement in terms of the coverage of each interval, especially when $p_2 = 5\%$. This approach effectively accounts for the uncertainty in the CRC estimators and provides a stable credible interval across a wide range of the sampling rate.

Table 3 Simulation result to compare the estimation for treatment A with $\mu_{true} = 0.68$, $N_{tot} = 1,000$

Setting	Estimation	$\hat{\mu}_1^a$	$\hat{\mu}_{RS}$	$\hat{\mu}_{Chap}^b$	$\hat{\mu}_{\Phi}^c$	$\hat{\mu}_{CRC}^c$
$p_2=5\%$	mean	0.752	0.678	0.673	0.678	0.677
	SD	0.019	0.097	0.149	0.072	0.074
	Avg.SE	0.019	0.091	0.132	0.067	0.066
	Width	0.075	0.357	0.446	0.262 (0.249)	0.258 (0.234)
	CI (%)	4.9	89.7	97.3	90.6 (95.4)	87.8 (94.5)
$p_2=10\%$	mean	0.751	0.681	0.679	0.681	0.680
	SD	0.019	0.064	0.098	0.049	0.050
	Avg.SE	0.020	0.065	0.096	0.049	0.048
	Width	0.077	0.256	0.369	0.190 (0.190)	0.189 (0.179)
	CI (%)	4.7	92.8	95.8	94.1 (95.6)	92.5 (94.7)
$p_2=20\%$	mean	0.751	0.681	0.679	0.680	0.680
	SD	0.020	0.047	0.070	0.037	0.037
	Avg.SE	0.020	0.046	0.066	0.035	0.035
	Width	0.079	0.182	0.253	0.139 (0.147)	0.139 (0.134)
	CI (%)	6.9	94.2	85.1	94.1 (94.3)	94.3 (94.4)

a. the estimation result based on Stream 1 only is reported for $\hat{\mu}_1$

b. the transformed logit CI³⁷ is reported for $\hat{\mu}_{Chap}$

c. the proposed Bayesian Credible Interval (**bold**) is reported for $\hat{\mu}_{\Phi}$ and $\hat{\mu}_{CRC}$

Table 4 Simulation result to compare the estimation for treatment B with $\mu_{true} = 0.54$, $N_{tot} = 1,000$

Setting	Estimation	$\hat{\mu}_1^a$	$\hat{\mu}_{RS}$	$\hat{\mu}_{Chap}^b$	$\hat{\mu}_{\Phi}^c$	$\hat{\mu}_{CRC}^c$
	mean	0.443	0.538	0.524	0.539	0.540

$p_2=5\%$	SD	0.029	0.101	0.252	0.084	0.084
	Avg.SE	0.029	0.098	0.217	0.081	0.079
	Width	0.113	0.383	0.665	0.316 (0.298)	0.308 (0.285)
	CI (%)	7.9	92.2	97.1	92.1 (95.7)	91.0 (94.9)
$p_2=10\%$	mean	0.442	0.541	0.545	0.542	0.542
	SD	0.030	0.071	0.207	0.060	0.060
	Avg.SE	0.029	0.070	0.171	0.058	0.057
	Width	0.115	0.273	0.572	0.228 (0.223)	0.223 (0.213)
$p_2=20\%$	CI (%)	8.2	93.9	95.1	93.6 (95.2)	92.6 (94.6)
	mean	0.442	0.541	0.539	0.540	0.540
	SD	0.030	0.049	0.129	0.043	0.043
	Avg.SE	0.030	0.050	0.118	0.042	0.041
	Width	0.118	0.194	0.442	0.164 (0.166)	0.162 (0.157)
CI (%)	9.7	94.7	91.1	93.9 (94.7)	93.8 (94.3)	

- the estimation result based on Stream 1 only is reported for $\hat{\mu}_1$
- the transformed logit CI³⁷ is reported for $\hat{\mu}_{Chap}$
- the proposed Bayesian Credible Interval (**bold**) is reported for $\hat{\mu}_{\hat{\varphi}}$ and $\hat{\mu}_{CRC}$

Results pertaining to the estimated outcome mean for treatment B are presented in **Table 4**, leading to qualitatively similar conclusions to those based on **Table 3**. Given the closely aligned performance of the two CRC estimators $\hat{\mu}_{\hat{\varphi}}$ and $\hat{\mu}_{CRC}$, either could be recommended in practice. However, it is worth noting that the estimator $\hat{\mu}_{CRC}$ tends to provide a narrower Bayesian credible interval compared to $\hat{\mu}_{\hat{\varphi}}$.

Table 5 Simulation result to compare the average treatment effect (ATE)^a with $ATE_{true} = 0.14$, $N_{tot} = 1,000$

Setting	Estimation	ATE_1^b	ATE_{RS}	ATE_{Chap}	$ATE_{\hat{\varphi}}^c$	ATE_{CRC}^c
$p_2=5\%$	Mean	0.309	0.139	0.150	0.139	0.138
	SD	0.035	0.140	0.292	0.112	0.113
	Avg.SE	0.035	0.134	0.267	0.105	0.103
	Width	0.136	0.524	1.047	0.412 (0.393)	0.404 (0.372)
	CI (%)	0.2	93.1	97.5	93.0 (95.0)	91.5 (94.2)
$p_2=10\%$	Mean	0.309	0.140	0.134	0.139	0.139
	SD	0.036	0.094	0.231	0.076	0.077
	Avg.SE	0.035	0.096	0.203	0.076	0.075
	Width	0.138	0.374	0.794	0.297 (0.294)	0.293 (0.278)
	CI (%)	0.3	95.3	95.2	94.9 (95.5)	93.5 (94.7)
$p_2=20\%$	Mean	0.310	0.140	0.140	0.140	0.140
	SD	0.037	0.068	0.147	0.055	0.055
	Avg.SE	0.036	0.068	0.137	0.055	0.054

	Width	0.141	0.266	0.538	0.215 (0.223)	0.213 (0.207)
	CI (%)	0.5	95.1	94.4	94.6 (94.7)	94.2 (94.5)

- the average treatment effects (ATE) equals to $\hat{\mu}_A - \hat{\mu}_B$
- the estimation result based on Stream 1 only is reported for $\hat{\mu}_1$
- the proposed adaptive Bayesian Credible Interval (**bold**) is reported for $ATE_{\hat{\varphi}}$ and ATE_{CRC}

In **Table 5**, we evaluate the Average Treatment Effect (ATE) based on the outcome means given in **Table 3** and **Table 4**. As expected, the estimate from the Stream 1 data is still biased due to its non-representativeness, while the other estimators are essentially unbiased. Notably, ATE_{Chap} suffers from slight bias here, as it loses some estimation accuracy due to zero-counts in some cells of **Table 1** when the sampling rate of stream 2 is small. However, the more serious problem is that Chapman’s estimator is highly inefficient in this setting. Overall, the proposed CRC estimators, $ATE_{\hat{\varphi}}$ and ATE_{CRC} , demonstrate the best performance for ATE estimation. In particular, ATE_{CRC} , together with the proposed Bayesian credible interval, provides the most reliable and precise estimation.

For the second simulation study to investigate treatment effects in terms of general means, we generated a continuous outcome \tilde{Y} characterized by heterogeneity in its distribution across members of the simulated target population. We adopt a mixture of varying normal distributions based on different strata, treatment binary response (Y) and treatment selection. Specifically, the continuous outcome \tilde{Y} is generated from eight different normal distributions with the combination of (i, j, k, μ, σ) , where $i = 1, 2$ for strata, $j = 1, 0$ for treatment binary response Y , $k = A, B$ for treatment selection, and mean and standard deviation μ, σ : $(1, 1, A, 10, 0.75)$, $(1, 0, A, 2.5, 1.2)$, $(2, 1, A, 5, 0.5)$, $(2, 0, A, 1, 1.5)$, $(1, 1, B, 15, 0.75)$, $(1, 0, B, 7.5, 1.2)$, $(2, 1, B, 10, 0.5)$, $(2, 0, B, 6, 1.5)$. Based on the weighted average of each normal distribution, the true overall mean of \tilde{Y} is therefore calculated as $\mu_A = 5.02$, $\mu_B = 9.18$. The true mean difference (treatment effect) follows, i.e., $\mu^{AB} = \mu_A - \mu_B = -4.16$.

The results of this simulation study with a population size ($N_{tot} = 1,000$) and sampling rate for Stream 2 ($p_2 = 10\%$) are summarized in **Table 6**. We examined the proposed mean estimators based on (8) and the treatment difference (ATE) between treatment groups A and B . For each estimator, we compared three distinct methods for assessing the mean of the continuous outcome \tilde{Y} . The “Stream 1 only” method derives the mean estimate solely from Stream 1 data. All estimates calculated in this way are biased due to the nonrepresentative sampling scheme of Stream 1. In contrast, the “Stream 2 only” method calculates the mean estimate exclusively from the anchor stream (Stream 2), yielding unbiased results as anticipated. Meanwhile, incorporating both Stream 1 and Stream 2 data, the “CRC” method reports more efficient mean estimates based on the capture-recapture framework. A more expanded set of simulation scenarios examining different sampling rate of Stream 2 ($p_2 = 5\%, 20\%$) can be found in the Appendix 4 of *Supplementary Document* (Tables S7-S8).

Table 6 Simulations Evaluating Mean Estimates for Continuous X with $N_{tot}=1000$, $p_2=10\%$

Estimator	True mean	Methods	Mean	SD	Average SE ^a	CI Coverage %	Average CI Width
$\hat{\mu}_A^b$	5.020	Stream 1 only	4.533	0.110	-	-	-
		Stream 2 only	5.036	0.431	0.423	94.4	1.646
		CRC	5.033	0.359	0.347	93.5	1.344
$\hat{\mu}_B^b$	9.180	Stream 1 only	9.414	0.190	-	-	-
		Stream 2 only	9.178	0.387	0.397	93.9	1.544
		CRC	9.181	0.323	0.316	93.1	1.231
$\hat{\mu}^{AB}$	-4.160	Stream 1 only	-4.880	0.216	-	-	-
		Stream 2 only	-4.141	0.586	0.581	94.6	2.262
		CRC	-4.147	0.493	0.471	93.6	1.832

a. SE for each estimator based on bootstrap with percentile CIs.

b. SE, CIs and its widths for the estimated mean not reported for the estimator based on Stream 1 only.

4. Illustrative Data Example

The design and estimation approaches outlined above demonstrated clear advantages for conducting causal inference in observational cohort studies, both conceptually and empirically, as

shown through the simulation studies. However, implementing such approaches in practice requires careful adherence to strict guidelines for random sampling and “*label-switching*”. Given the newly proposed CRC framework for causal inference, we present an illustrative data example using two research studies comparing the antibody response to two Covid-19 vaccines.

Beginning in early 2020, a newly discovered coronavirus, Severe Acute Respiratory Syndrome Coronavirus 2 (SARS-CoV-2), spread worldwide. In response, healthcare experts and pharmaceutical companies worked collaboratively to develop vaccines to combat the virus. To date, numerous studies⁴²⁻⁴⁴ have compared different vaccines, focusing on major Covid-19 vaccines such as mRNA-1273 (Moderna), BNT162B2 (Pfizer-BioNTech), Sputnik V (Gamaleya Research Institute), ChAdOx1-S (AstraZeneca), Sinopharm (BIBP), and Sinovac (Beijing). Most of these studies^{42,43} are observational, examining vaccine effectiveness, efficacy, and antibody responses (seropositivity). However, the generalizability of these findings is often questioned due to selection bias. A smaller number of studies include randomized trials, although their limited sample sizes present challenges.

This article introduces a method for integrating data from both study types to strengthen inferences. We illustrate this approach by mimicking a randomized trial from Tunisia⁴⁴ and generating synthetic observational data purportedly from the same target population under a capture-recapture framework. In this example, we compare antibody responses following two doses of hypothetical treatment modeled after the Sputnik V and Sinopharm vaccines.

As of 12 January 2022, over 6 million individuals in Tunisia had completed vaccination with one of the common Covid-19 vaccines.⁴⁴ The synthetic target population for this example comprises 2,000 hypothetical Tunisians aged 40 and older who had not experienced symptomatic Covid-19 and had provided informed consent for vaccination. Following the study design outlined

above, we assume participants received the vaccine of their choice or as recommended by their medical providers, after which their humoral antibody responses (Anti-S Antibodies) were assessed using a commercial Anti-SARS-CoV-2 test following the second dose. For this demonstration, test results on a random sample from the actual Tunisian target population (including 169 participants⁴⁴, representing 8.45% of the 2,000 individuals) were used to set parameters for generating anchor stream data to be combined with the synthetic observational data. We use synthetic individual-level data to emulate the target population in Tunisia by randomly sampling data until acquiring 85 seropositive responses for *A* and 71 for *B* among 169 random samples to mimic Stream 2 data based on Ahmed et al.⁴⁴, serving as the anchor stream. **Table 7** presents the number and percentage of seropositive individuals in these empirical studies.

Table 7 Number and percent of seropositive participants for two vaccine types in Tunisia

Vaccine	Stream 1 ^a		Stream 2 ^b	
	N	Seropositive (%)	N	Seropositive (%)
Vaccine <i>A</i>	327	293 (89.6%)	86	85 (98.8%)
Vaccine <i>B</i>	571	508 (89.0%)	83	71 (85.5%)
Total	898	-	169	-

a. Stream 1 comprises synthetic data from observational cohorts. The total target population size is N=2,000.

b. Stream 2 mimics randomized trial cohorts from Ahmed et al.⁴⁴ Vaccine *A* represents Sputnik V, while Vaccine *B* represent Sinopharm.

For a synthetic target population, we assume that vaccine selection was associated with a variable such as insurance type, where older individuals and/or those of lower socioeconomic status might be covered by one type of insurance (comprising 5% of the population, with 90% receiving Vaccine *A* showing a seropositivity rate of 75%, and the rest receiving Vaccine *B* with a seropositivity rate of 60%). In contrast, younger or more affluent individuals might use another type of insurance (comprising 95% of the population, with 30% receiving Vaccine *A* showing a seropositivity rate of 99%, and the remainder receiving Vaccine *B* with a seropositivity rate of 90%). As a result, the true seropositivity rates were set at 97.8% for Vaccine *A* and 88.5% Vaccine

B. In the synthetic observational cohort (Stream 1), the vast majority (99%) of subjects with the first type of insurance participated, while those with the second type had a lower participation rate (45%), reflecting a logical source of potential non-representativeness.

Table 8 Seropositivity Estimates and Comparison for the Synthetic Population in Tunisia ^a

Vaccine	Estimator	Mean	SE	95% CI ^b	Width
Vaccine A	$\hat{\mu}_{RS,A}$	98.8%	0.0116	[96.6%, 100.0%]	0.034 ^c
	$\hat{\mu}_{CRC,A}$	98.0%	0.0059	[96.8%, 99.1%], [95.4%, 98.4%]	0.023, 0.029
Vaccine B	$\hat{\mu}_{RS,B}$	85.5%	0.0386	[78.0%, 93.1%]	0.151
	$\hat{\mu}_{CRC,B}$	88.5%	0.0292	[82.8%, 94.3%], [81.8%, 93.0%]	0.114, 0.112
Difference ^d	ATE_1	0.6%	0.0213	[0.0%, 4.8%]	0.048
	ATE_{RS}	13.3%	0.0403	[5.4%, 21.2%]	0.158
	ATE_{CRC}	9.5%	0.0298	[3.6%, 15.3%], [3.7%, 16.4%]	0.117, 0.127

a. In this example, the true seropositivity rates were set at 97.8% for Vaccine A and 88.5% Vaccine B.

b. The Wald-based CIs reported for $\hat{\mu}_{RS,A}$ and $\hat{\mu}_{RS,B}$ are based on the random sampling estimator given in eqn. (1); The Wald-based CIs reported for $\hat{\mu}_{CRC,A}$ and $\hat{\mu}_{CRC,B}$ are based on the variance estimator for eqn. (3) and (4) given in *Appendix 3*; The proposed Bayesian Credible Intervals (**bold**) reported for $\hat{\mu}_{CRC,A}$ and $\hat{\mu}_{CRC,B}$ are based on Section 2.4;

c. The upper limit of the CI for $\hat{\mu}_{RS,A}$ is capped at 100%, with a width of 0.045 when disregarding the cap.

d. The difference of two vaccines equals to $\hat{\mu}_{RS,A} - \hat{\mu}_{RS,B}$ or $\hat{\mu}_{CRC,A} - \hat{\mu}_{CRC,B}$, which matches the definition of *ATE* introduced in previous sections. ATE_1 is reported for the comparison based on Stream 1 only.

For illustration, a single set of observed cell counts (see **Table 2**) was simulated as follows:

$n_1=12, n_2=1, n_3=281, n_4=33, n_5=33, n_6=0, n_7=18, n_8=5, n_9=490, n_{10}=58, n_{11}=14, n_{12}=2, n_{13}=40, n_{14}=0, n_{15}=39, n_{16}=5, n_{17}=969$, corresponding to the counts in Table 7, e.g., the cell count for positive responses to Vaccine A in Stream 1 is $n_{S1}^A = n_1 + n_3 = 293$, and in Stream 2 it is $n_{S2}^A = n_1 + n_5 + n_{13} = 85$. We then compare the CRC estimator $\hat{\mu}_{CRC}$ based on eqns. (3) and (4) to the random sampling estimator $\hat{\mu}_{RS}$ derived from the randomized trial data. The results of this example are presented in **Table 8**. Vaccine A and Vaccine B, representing the two Covid-19 vaccines mentioned earlier, illustrate seropositivity estimates within the synthetic population. As anticipated, leveraging additional information from the observational cohorts provides significant

benefits, such as reducing interval widths by approximately 20% (e.g., from 0.158 to 0.127 for ATE_{CRC}), consistent with conclusions drawn from the simulation studies. Furthermore, the difference in seropositivity rates estimated based on Stream 1 (ATE_1) is biased toward the null, clearly highlighting the common issue of selection bias inherent in observational data. Although only a single set of simulated data is presented, the Stream 2 data are exactly representative of the Tunisian trial.⁴⁴ A reliability analysis is also provided in Appendix 5 of *Supplementary Document*, to demonstrate the robustness of this example as it applies to real-world data practice.

Additionally, most antibody comparison studies^{42–44} focus on comparing both the binary seropositivity response and continuous measurements of antibody levels, such as cellular immune responses based on CD4 or CD8 levels. The extension introduced in Section 2.5 is well suited for this context. However, due to the lack of relevant data, our illustrative example only addresses comparisons of seropositive response rate (binary outcomes). Given availability of continuous outcome data, the proposed method can be readily applied to address such research interests.

5. Discussion

In this article, we have employed capture-recapture methods to evaluate treatment effects and extend causal inference from an observational study to a trial-eligible target population. We have introduced several estimators to evaluate the response probabilities for the individual treatments, as well as the average treatment effect (ATE). Our empirical studies suggest that the proposed anchor stream-based estimators provide unbiased and efficient estimation for the outcome mean of a single treatment as well as the ATE, with enhanced precision compared to the random sampling-based estimator. As an application, we demonstrated our method using an illustrative example based on a randomized trial from Tunisia, comparing Anti-S Antibody seropositive response rates between two major Covid-19 vaccines and yielding conclusions consistent with

those from the empirical studies. All R programs related to the simulation studies and the illustrative data example are available on GitHub (https://github.com/lge-biostat/CRC_causal_inference).

In the causal inference literature, researchers often consider the transportability of causal conclusions from observational studies and examine the generalizability of findings from randomized trials. This is because the advantages and disadvantages of each approach can affect either the internal or external validity⁴. In both the observational study and randomized trial, the causal conclusion is evaluated based on a study sample and extended from a subpopulation sample to the target population. In the CRC analysis considered in this work, missing information is estimated based on observed information, and therefore the causal conclusion made via CRC focuses on the entire target population instead of just the study sample. Specifically, the proposed anchor stream-based CRC estimators leverage the generalizability of the representative sample and “transport” the observational information to improve precision, which may offer a novel approach in the area of causal inference when the design can be implemented.

Our approach to performing the CRC analysis proposed here relies on the study design introduced in Section 1 and requires the capacity to draw a representative sample from a well-defined target population that consists of a list or registry of individuals eligible for treatment assessment. Similar study designs exist for combining randomized trials and observational studies, such as pragmatic randomized trials nested within a cohort of eligible individuals^{45,46}. These designs assume that the observational data can provide a good representative basis for the randomized trial, and that inference based on an embedded randomized trial could improve the generalizability and transportability. However, in our approach, we do not make any assumptions about the nature of the non-representativeness characterizing the observational study participants,

as this is often unverifiable in practice⁴⁷. Instead, we leverage what can be a much smaller representative random sample from the target population to anchor the estimation validity, while borrowing added precision from the observational component. Future work may consider extending the causal conclusions from the trial-eligible target population to a more general target population. To achieve this goal, baseline covariate information may need to be considered, and a stratified sampling approach to acquire the anchor stream may be necessary. We also anticipate generalization of the measure of treatment effect considered here, as well as potential efforts to target favorable bias-variance tradeoffs if covariates deemed to explain the majority of the observational non-representativeness are available.

Acknowledgements

This work was supported by the National Institute of Health (NIH)/National Institute of Allergy and Infectious Diseases (P30AI050409; Del Rio PI), the NIH/National Center for Advancing Translational Sciences (UL1TR002378; Taylor PI), the NIH/National Cancer Institute (R01CA234538; Ward/Lash MPIs), and the NIH/National Cancer Institute (R01CA266574; Lyles/Waller MPIs).

References

1. Colnet B, Mayer I, Chen G, et al. Causal inference methods for combining randomized trials and observational studies: a review. Published online November 16, 2020. doi:10.48550/arxiv.2011.08047
2. D'Agostino RB. Propensity score methods for bias reduction in the comparison of a treatment to a non-randomized control group. *Stat Med*. Published online 1998. doi:10.1002/(SICI)1097-0258(19981015)17:19<2265::AID-SIM918>3.0.CO;2-B
3. Robins JM, Rotnitzky A, Zhao LP. Estimation of regression coefficients when some regressors are not always observed. *J Am Stat Assoc*. Published online 1994. doi:10.1080/01621459.1994.10476818
4. Degtiar I, Rose S. A Review of Generalizability and Transportability. *Annu Rev Stat Appl*. 2023;10(1):501-524. doi:10.1146/annurev-statistics-042522-103837
5. Rothwell PM. External validity of randomized controlled trials: “to whom do the results of this trial apply?” *Lancet*. Published online 2005. doi:10.1016/S0140-6736(04)17670-8
6. Dahabreh IJ, Robertson SE, Tchetgen EJ, Stuart EA, Hernán MA. Generalizing causal inferences from individuals in randomized trials to all trial-eligible individuals. *Biometrics*. Published online 2019. doi:10.1111/biom.13009
7. Stuart EA, Ackerman B, Westreich D. Generalizability of Randomized Trial Results to Target Populations: Design and Analysis Possibilities. *Res Soc Work Pract*. Published online 2018. doi:10.1177/1049731517720730
8. Bareinboim E, Pearl J. A General Algorithm for Deciding Transportability of Experimental Results. *J Causal Inference*. Published online 2013. doi:10.1515/jci-2012-0004

9. Hernán MA, Vanderweele TJ. Compound treatments and transportability of causal inference. *Epidemiology*. Published online 2011. doi:10.1097/EDE.0b013e3182109296
10. Borchers DL. *Estimating Animal Abundance: Closed Populations (Statistics for Biology and Health)*.; 2002.
11. Chao A. An overview of closed capture-recapture models. *J Agric Biol Environ Stat*. Published online 2001. doi:10.1198/108571101750524670
12. Poorolajal J, Mohammadi Y, Farzinara F. Using the capture-recapture method to estimate the human immunodeficiency virus-positive population. *Epidemiol Health*. Published online 2017. doi:10.4178/epih.e2017042
13. Wu C, Chang HG, McNutt LA, Smith PF. Estimating the mortality rate of hepatitis C using multiple data sources. *Epidemiol Infect*. Published online 2005. doi:10.1017/S0950268804003103
14. Dunbar R, Van Hest R, Lawrence K, et al. Capture-recapture to estimate completeness of tuberculosis surveillance in two communities in South Africa. *International Journal of Tuberculosis and Lung Disease*. Published online 2011. doi:10.5588/ijtld.10.0695
15. Frischer M, Bloor M, Finlay A, et al. A new method of estimating prevalence of injecting drug use in an urban population: Results from a Scottish city. *Int J Epidemiol*. Published online 1991. doi:10.1093/ije/20.4.997
16. Lyles RH, Zhang Y, Ge L, Waller LA. A Design and Analytical Strategy for Monitoring Disease Positivity and Biomarker Levels in Accessible Closed Populations. *Am J Epidemiol*. 2024;193(1):193-202.

17. Zhang Y, Chen J, Ge L, Williamson JM, Waller LA, Lyles RH. Sensitivity and Uncertainty Analysis for Two-Stream Capture-Recapture Methods in Disease Surveillance. *Epidemiology*. Published online March 27, 2023. doi:10.1097/EDE.0000000000001614
18. Zhang B, Small DS. Number of healthcare workers who have died of COVID-19. *Epidemiology*. Published online 2020. doi:10.1097/EDE.0000000000001229
19. Chao A, Pan HY, Chiang SC. The Petersen - Lincoln estimator and its extension to estimate the size of a shared population. *Biometrical Journal*. Published online 2008. doi:10.1002/bimj.200810482
20. Brenner H. Use and limitations of the capture-recapture method in disease monitoring with two dependent sources. *Epidemiology*. Published online 1995. doi:10.1097/00001648-199501000-00009
21. G. M. Book received. G. A. F. Seber, 1982: The estimation of animal abundance and related parameters. London, Charles Griffin & Co. Ltd. 654 pp. *Acta Theriol (Warsz)*. Published online 1982. doi:10.4098/at.arch.82-33
22. Seber GAF. A Review of Estimating Animal Abundance. *Biometrics*. Published online 1986. doi:10.2307/2531049
23. Lyles RH, Zhang Y, Ge L, et al. Using Capture–Recapture Methodology to Enhance Precision of Representative Sampling-Based Case Count Estimates. *J Surv Stat Methodol*. Published online 2022. doi:10.1093/jssam/smab052
24. Ge L, Zhang Y, Ward KC, Lash TL, Waller LA, Lyles RH. Tailoring Capture-Recapture Methods to Estimate Registry-Based Case Counts Based on Error-Prone Diagnostic Signals. *Stat Med*. 2023;42(17):2928–2943. doi:10.1002/sim.9759

25. Cook C, Sheets C. Clinical equipoise and personal equipoise: Two necessary ingredients for reducing bias in manual therapy trials. *Journal of Manual and Manipulative Therapy*. Published online 2011. doi:10.1179/106698111X12899036752014
26. Kukla R. Resituating the principle of equipoise: Justice and access to care in non-ideal conditions. *Kennedy Inst Ethics J*. Published online 2007. doi:10.1353/ken.2007.0014
27. Sando D, Geldsetzer P, Magesa L, et al. Evaluation of a community health worker intervention and the World Health Organization's Option B versus Option A to improve antenatal care and PMTCT outcomes in Dar es Salaam, Tanzania: Study protocol for a cluster-randomized controlled health systems implementation trial. *Trials*. 2014;15(1):1-13. doi:10.1186/1745-6215-15-359/FIGURES/1
28. Shadish WR, Cook TD, Campbell DT. *Experimental and Quasi-Experimental Designs for Generalized Causal Inference*. Boston: Houghton Mifflin.; 2002.
29. Olsen RB, Orr LL. On the "Where" of Social Experiments: Selecting More Representative Samples to Inform Policy. *New Dir Eval*. Published online 2016. doi:10.1002/ev.20207
30. Rubin DB. Estimating causal effects of treatments in randomized and nonrandomized studies. *J Educ Psychol*. Published online 1974. doi:10.1037/h0037350
31. Splawa-Neyman J. On the application of probability theory to agricultural experiments. Essay on principles. Section 9. *Statistical Science*. Published online 1990. doi:10.1214/ss/1177012031
32. Robins JM, Greenland S. Causal Inference Without Counterfactuals: Comment. *J Am Stat Assoc*. Published online 2000. doi:10.2307/2669381

33. Ge L, Zhang Y, Waller LA, Lyles RH. Enhanced Inference for Finite Population Sampling-Based Prevalence Estimation with Misclassification Errors. *Am Stat*. Published online August 23, 2023;1-11. doi:10.1080/00031305.2023.2250401
34. Petersen CGJ. The yearly immigration of young plaice into the Limfjord from the German Sea, ect. *Report of the Danish Biological Station for 1985*. 1986;6:1-48. Accessed January 24, 2023. <https://cir.nii.ac.jp/crid/1571135650073221120.bib?lang=en>
35. Lincoln FC. Calculating waterfowl abundance on the basis of banding returns. *US Department of Agriculture*. Published online 1930.
36. Chapman DG. *Some Properties of the Hypergeometric Distribution with Applications to Zoological Sample Censuses*. Berkeley, University of California Press; 1951.
37. Sadinle M. Transformed logit confidence intervals for small populations in single capture-recapture estimation. *Commun Stat Simul Comput*. Published online 2009. doi:10.1080/03610910903168595
38. Agresti A, Coull BA. Approximate is better than “Exact” for interval estimation of binomial proportions. *American Statistician*. Published online 1998. doi:10.1080/00031305.1998.10480550
39. Brown LD, Cai TT, Das Gupta A. Interval estimation for a binomial proportion. *Statistical Science*. Published online 2001. doi:10.1214/ss/1009213286
40. Naing NN. Easy way to learn standardization : direct and indirect methods. *Malays J Med Sci*. Published online 2000.
41. Efron B, Tibshirani RJ. *An Introduction to the Bootstrap.*; 1994. doi:10.1201/9780429246593

42. Jeewandara C, Aberathna IS, Danasekara S, et al. Comparison of the immunogenicity of five COVID-19 vaccines in Sri Lanka. *Immunology*. Published online 2022. doi:10.1111/imm.13535
43. Mok CKP, Cohen CA, Cheng SMS, et al. Comparison of the immunogenicity of BNT162b2 and CoronaVac COVID-19 vaccines in Hong Kong. *Respirology*. Published online 2022. doi:10.1111/resp.14191
44. Ben Ahmed M, Bellali H, Gdoura M, et al. Humoral and Cellular Immunogenicity of Six Different Vaccines against SARS-CoV-2 in Adults: A Comparative Study in Tunisia (North Africa). *Vaccines (Basel)*. Published online 2022. doi:10.3390/vaccines10081189
45. Ford I, Norrie J. Pragmatic Trials. *New England Journal of Medicine*. Published online 2016. doi:10.1056/nejmra1510059
46. Newman AB, Avilés-Santa ML, Anderson G, et al. Embedding clinical interventions into observational studies. *Contemp Clin Trials*. Published online 2016. doi:10.1016/j.cct.2015.11.017
47. Hammer GP, Prel JB du, Blettner M. Avoiding Bias in Observational Studies. *Dtsch Arztebl Int*. Published online 2009. doi:10.3238/arztebl.2009.0664